

Pilot evaluation of long-term reproducibility of capillary zone electrophoresis-tandem mass spectrometry for top-down proteomics of a complex proteome sample

Seyed Amirhossein Sadeghi,¹ Wenrong Chen,² Qianyi Wang,¹ Qianjie Wang,¹ Fei Fang,¹ Xiaowen Liu,³ Liangliang Sun^{1,*}

¹Department of Chemistry, Michigan State University, 578 S Shaw Lane, East Lansing, Michigan 48824, USA

²Department of BioHealth Informatics, Indiana University-Purdue University Indianapolis, 535 W Michigan Street, Indianapolis, IN 46202, USA

³Deming Department of Medicine, School of Medicine, Tulane University, 1441 Canal Street, New Orleans, LA 70112, USA

* Corresponding Author. Email: lsun@chemistry.msu.edu

Phone: 517-353-0498

1

2 **Abstract**

3 Mass spectrometry (MS)-based top-down proteomics (TDP) has revolutionized biological
4 research by measuring intact proteoforms in cells, tissues, and biofluids. Capillary zone
5 electrophoresis-tandem MS (CZE-MS/MS) is a valuable technique for TDP, offering high
6 peak capacity and sensitivity for proteoform separation and detection. However, the long-
7 term reproducibility of CZE-MS/MS in TDP remains unstudied, a crucial aspect for large-
8 scale studies. This work investigated the long-term qualitative and quantitative
9 reproducibility of CZE-MS/MS for TDP for the first time, focusing on a yeast cell lysate.
10 Over 1000 proteoforms were identified per run across 62 runs using one linear
11 polyacrylamide (LPA)-coated separation capillary, highlighting the robustness of the CZE-
12 MS/MS technique. However, substantial decreases in proteoform intensity and
13 identification were observed after some initial runs due to proteoform adsorption onto the
14 capillary inner wall. To address this issue, we developed an efficient capillary cleanup
15 procedure using diluted ammonium hydroxide, achieving high qualitative and quantitative
16 reproducibility for the yeast sample across at least 23 runs. The data underscores the
17 capability of CZE-MS/MS for large-scale quantitative TDP of complex samples, signaling
18 its readiness for deployment in broad biological applications. The MS RAW files were
19 deposited in ProteomeXchange Consortium with the dataset identifier of PXD046651.

20 **KEYWORDS:** top-down proteomics, capillary zone electrophoresis, mass spectrometry,
21 proteoform, reproducibility, label-free quantification, yeast cell lysate

22

23

24

25

26

1 **Introduction**

2 Mass spectrometry (MS)-based top-down proteomics (TDP) is a powerful technique for
3 the identification and quantification of proteoforms in biological samples¹. During the last
4 several years, TDP has been deployed widely to discover new proteoform biomarkers of
5 various diseases, e.g., cancer²⁻⁵, neurodegeneration⁶⁻⁹, cardiovascular diseases¹⁰,
6 infectious disease¹¹⁻¹⁴, and immunobiology¹⁵. MS-based TDP is providing more and more
7 new insights into the functions of proteins in modulating the cellular processes.

8 Due to the high complexity of the proteoforms in cells or tissues, high peak capacity
9 separations of proteoforms before MS is crucial. Liquid chromatography (LC)-MS has
10 been the widely used technique for TDP of complex samples^{16,17}. Capillary zone
11 electrophoresis (CZE) offers highly efficient separations of biomolecules according to
12 electrophoretic mobility (μ_{ef}), which relates to their charge-to-size ratios¹⁸. CZE-MS has
13 also been well recognized as an alternative technique to LC-MS for global TDP profiling
14 of proteoforms in cells and tissues due to its high efficiency and sensitivity for proteoform
15 separation and detection as well as its unique opportunity for accurate prediction of
16 proteoform's μ_{ef} ¹⁹⁻²¹. Several research groups have shown the early examples of CZE-
17 MS for highly sensitive and global TDP of complex biological samples²²⁻²⁵. Our group
18 has shown the identification of hundreds to thousands of proteoforms from complex
19 samples by single-shot CZE-MS measurements via innovations in capillary coating,
20 online proteoform stacking, and etc^{19,20,26}. We further boosted the number of identified
21 proteoforms from human cell lines to over 23,000 by coupling LC fractionation to CZE-
22 MS³. Most recently, we developed online two dimensional FAIMS (high-field asymmetric
23 waveform ion mobility spectrometry)-CZE-MS to benefit the identification of large
24 proteoforms²⁷ and histone proteoforms²⁸. We also showed the capability of CZE-MS for
25 TDP of membrane proteins²⁹. The Kelleher group documented the high sensitivity of CZE-
26 MS for TDP and the reasonable complementarity between CZE-MS and LC-MS for
27 proteoform identification³⁰. The Ivanov group illustrated the potential of CZE-MS for TDP
28 of single mammalian cells³¹.

1 CZE-MS has made drastic progress in TDP and has been widely accepted as a useful
2 tool for proteoform characterization. However, to use CZE-MS for large-scale TDP
3 studies, we need to validate its long-term reproducibility for top-down MS measurement
4 of complex samples. In this work, for the first time, we performed a pilot investigation of
5 long-term reproducibility of CZE-MS for TDP of a complex sample (i.e., a yeast cell lysate)
6 to achieve a better understanding of advantages, issues, and potential solutions of CZE-
7 MS for large-scale TDP.

8 **EXPERIMENTAL SECTION**

9 **Chemicals and materials**

10 Ammonium bicarbonate (ABC), ammonium hydroxide (NH₄OH), 3-(trimethoxysilyl) propyl
11 methacrylate, and Amicon Ultra (0.5 mL, 10 kDa cut-off size) centrifugal filter units and
12 (Yeast Extract–Peptone–Dextrose) YPD Broth were ordered from Sigma-Aldrich (St.
13 Louis, MO). LC/ MS grade water, acetonitrile (ACN), HPLC-grade acetic acid (AA), fused
14 silica capillaries (50 mm i.d., 360 mm o.d., Polymicro Technologies) were purchased from
15 Fisher Scientific (Pittsburgh, PA). Acrylamide was obtained from Acros Organics (Fair
16 Lawn, NJ). Complete, mini protease inhibitor cocktail (provided in EASYpacks) was
17 bought from Roche (Indianapolis, IN).

18 **Sample preparation**

19 Yeast growth in (Yeast Extract–Peptone–Dextrose) YPD Broth is meticulously cultivated
20 using a well-defined procedure. To begin, 50 g of YPD Broth was blended with 1 liter of
21 distilled water, ensuring a precise mixture. This suspension underwent autoclaving at
22 121°C for a duration of 15 minutes. Following this, yeast cultures are introduced into
23 detergent-free containers. A brief vortexing was then carried out to uniformly disperse the
24 yeast cells throughout the medium. The yeast cultures were subsequently nurtured in a
25 shaking incubator at 300 rpm.

26 After yeast cell collection and cleanup with a PBS buffer, five gram of yeast cells were
27 suspended into the lysis buffer containing 8 M urea, complete protease inhibitors and
28 PhosSTOP (Roche), and 100 mM ammonium bicarbonate (pH 8.0), followed by

1 incubation on ice for 30 min with periodical vortexing. The cells were lysed for 3 min using
2 a homogenizer (Fisher Scientific) and then sonicated under 50% duty cycle, level 10
3 output for 20 min on ice with a Branson Sonifier 250 (VWR Scientific). The yeast lysate
4 was centrifuged at 14,000 g for 10 minutes at 4 °C to collect the supernatant containing
5 extracted proteins. The concentration of total proteins was measured by a bicinchoninic
6 acid (BCA) kit (Fisher Scientific) according to manufacturer's instructions and the sample
7 was stored at -80°C.

8 **Buffer exchange**

9 In this study, an Amicon Ultra Centrifugal Filter (Sigma Aldrich) with a Molecular Weight
10 Cut-Off (MWCO) of 10 kDa was utilized for buffer exchange to eliminate the urea
11 effectively from protein samples. The procedure began with the initial wetting of the filter
12 using 20 µL of 100 mM ammonium bicarbonate, followed by centrifugation at 14,000 g for
13 10 min. Subsequently, an aliquot of 200 µg proteins was added to the filter, and
14 centrifugation was carried out for 20 min at 14,000 g. 200 µL of 100 mM ammonium
15 bicarbonate was added to the filter, followed by centrifugation at 14,000 g for 20 min. This
16 step was repeated twice to remove the urea and other small interferences completely.
17 The final protein solution in 35 µL of 100 mM ammonium bicarbonate (protein
18 concentration was 3 mg/mL) was collected for CZE-MS analysis. All centrifugation steps
19 were performed at 4°C.

20 **Preparation of linear polyacrylamide (LPA)-coated capillary**

21 An LPA-coated capillary (1 meter, 50 µm i.d., 360 µm o.d.) was prepared according to
22 our previous procedure with minor modifications.³² First, 3 µL of ammonium persulfate
23 (APS) solution (5% [w/v] in water) was added to 500 µL of acrylamide solution (4% [w/v]
24 in water) and the mixture was degassed with nitrogen gas for 5 min to remove the oxygen
25 in the solution. Then, the mixture was loaded into the pretreated capillary using a vacuum,
26 followed by sealing both ends of the capillary with silica rubber, and incubating it in a
27 water bath at 50 °C for 40 min. Finally, a small portion (~5 mm) of the capillary from both
28 ends was removed with a cleaving stone and the unreacted solution (an agarose gel-like
29 consistency) was pushed out of the capillary with water (200 µL), using the syringe pump.

1 One end of the separation capillary was etched by hydrofluoric acid to reduce its outer
2 diameter to around 100 μm ³³.

3 **CZE-ESI-MS/MS Analysis**

4 The automated CE operation was performed using an ECE-001 CE autosampler from
5 CMP Scientific (Brooklyn, NY). Through an electro-kinetically pumped sheath flow CE-
6 MS interface (CMP Scientific, Brooklyn, NY), the CE system was coupled to a Q-Exactive
7 HF mass spectrometer (Thermo Fisher Scientific) ^{34,35}. For CZE separation, the LPA-
8 coated capillary (50 μm i.d., 360 μm o.d., 1 meter in length) was used. A background
9 electrolyte (BGE) of 5% (v/v) acetic acid (pH 2.4) was used for CZE. The sample buffer
10 was 100 mM ammonium bicarbonate (pH 8). The dramatic difference of BGE and sample
11 buffer in pH enabled online dynamic pH junction-based sample stacking.²⁶ The sheath
12 buffer contained 0.2% (v/v) formic acid and 10% (v/v) methanol. The sample was injected
13 into the capillary via applying pressure. The sample injection volume was calculated
14 based on the pressure and injection time using Poiseuille's Law. In this study, 5 psi for a
15 20-s period was applied for sample injection, corresponding to about 100 nL of sample-
16 loading volume for a 1-m-long separation capillary (50- μm i.d.). At the injection end of the
17 separation capillary, a high voltage (30 kV) was applied for separation, and in the sheath
18 buffer vial, a voltage of 2–2.2 kV was applied for ESI. With a Sutter P-1000 flaming/brown
19 micropipet puller, ESI emitters were pulled from borosilicate glass capillaries (1.0 mm
20 o.d., 0.75 mm i.d., and 10 cm length). ESI emitters had an opening size of 25 to 35 μm .

21 All experiments were conducted using the Q-Exactive HF mass spectrometer. A Data-
22 dependent acquisition (DDA) method was used for the
23 yeast protein sample. MS parameters were 120,000 mass resolution (at m/z 200), three
24 microscans, 3E6 AGC target value, 100 ms maximum injection time, and 600–2000 m/z
25 scan range. For MS/MS, 60,000 mass resolution (at 200 m/z), 1 microscan, 1E6 AGC,
26 200 ms injection time, 4 m/z isolation window, and 20% normalized collision energy (NCE)
27 were used. The top 8 most intense precursor ions in one MS spectrum were isolated in
28 the quadropole and fragmented via higher energy collision dissociation (HCD).
29 Fragmentation was performed only on ions with intensities greater than 1E4 and charge

1 states greater than 5. We enabled dynamic exclusion with a duration of 30 s. The
2 "Exclude isotopes" function was enabled.

3 **Data analysis**

4 The complex sample data was analyzed using Xcalibur software (Thermo Fisher
5 Scientific) to get intensity and migration time of proteins. For the final figures, the
6 electropherograms were exported from Xcalibur and formatted using Adobe Illustrator.

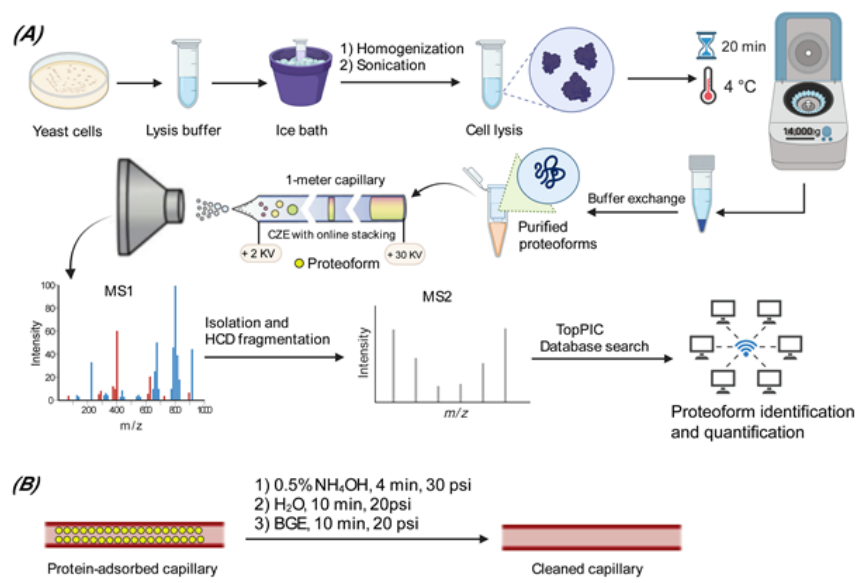
7 Proteoform identification and quantification were performed on the yeast protein RAW
8 files using the TopPIC (Top-down mass spectrometry-based Proteoform Identification
9 and Characterization) pipeline³⁶. In the first step, RAW files were converted into mzML
10 files using the Msconvert tool³⁷. The spectral deconvolution which converted precursor
11 and fragment isotope clusters into the monoisotopic masses and proteoform features
12 were then performed using TopFD (Top-down mass spectrometry Feature Detection,
13 version 1.5.6)³⁸. The resulting mass spectra and proteoform feature information were
14 stored in msalign and text files, respectively. The database search was performed using
15 TopPIC (version 1.5.6) against UniProt proteome database of Yeast (UP000002311,
16 6060 entries, version 11/14/2022) concatenated with a shuffled decoy database of the
17 same size of the yeast database. The maximum number of unexpected mass shifts was
18 one. The mass error tolerances for precursors and fragments were 15 parts-per-million
19 (ppm). There was a maximum mass shift of 500 Da for unknown mass shifts. To estimate
20 false discovery rates (FDRs) of proteoform identifications, the target-decoy approach
21 was used and proteoform identifications were filtered by a 1% FDR at the proteoform-
22 spectrum-match (PrSM) level and proteoform level^{39,40}. The lists of identified
23 proteoforms from all CZE-MS/MS runs are shown in **Supporting Information I**. The
24 TopDiff (Top-down mass spectrometry-based identification of Differentially expressed
25 proteoforms, version 1.5.6) software was used to perform label-free quantification of
26 identified proteoforms by CZE-MS/MS using default settings⁴¹. The MS RAW files were
27 deposited to the ProteomeXchange Consortium via the PRIDE⁴²partner repository with
28 the dataset identifier of PXD046651.

29 **Capillary cleanup**

1 To remove proteins adsorbed on the capillary inner wall, the capillary was cleaned
2 periodically by flushing with 0.5% NH₄OH for 10 minutes at 30 psi, H₂O for 10 min at 20
3 psi, and the BGE (5% acetic acid) for 10 min at 20 psi successively.

4 Results and discussion

5 For the first time, we studied long-term reproducibility of CZE-MS/MS for TDP of a
6 complex proteome sample, a yeast cell lysate, and developed an effective procedure for
7 cleaning up the inner wall of LPA coated capillaries for reproducible CZE-MS/MS
8 measurements of proteoforms. **Figure 1A** shows the experimental design of this project.
9 Yeast cells were lysed by homogenization and sonication. The proteoform extract was
10 analyzed by the dynamic pH junction-based CZE-MS/MS²⁶ after a simple buffer exchange
11 with a 10-kDa cut-off centrifugal filter unit. The yeast cell lysate was diluted to 1 mg/mL
12 with 100 mM ammonium bicarbonate (pH 8) for CZE-MS/MS. Finally, the TopPIC
13 software developed by the Liu's group was used for database search to identify and
14 quantify proteoforms. **Figure 1B** represents the clean-up procedure to remove the
15 adsorbed proteoforms on the LPA polymer coating on the capillary inner wall.



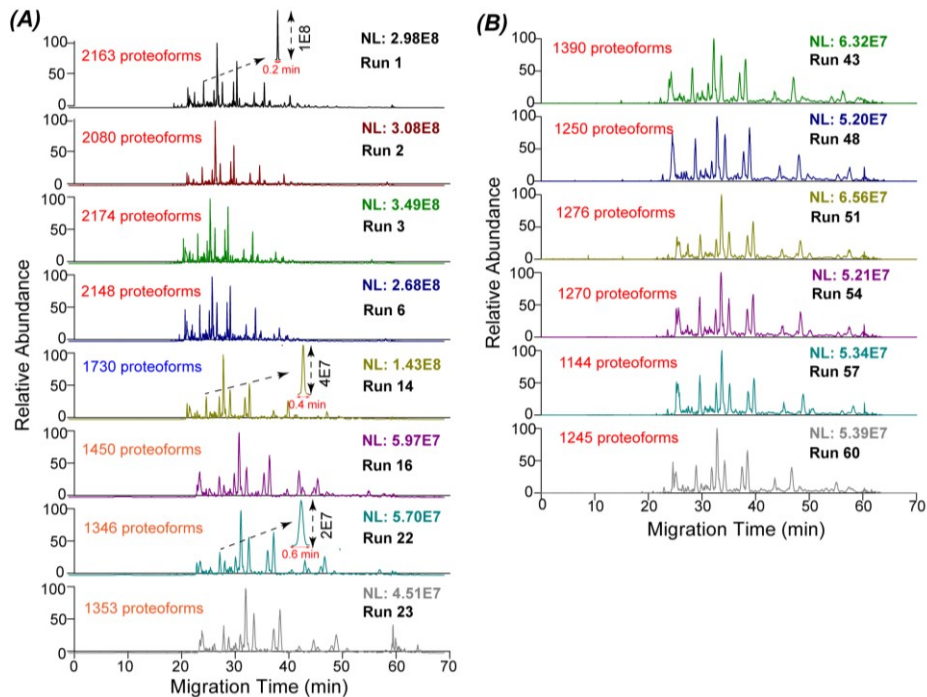
16

17 **Figure 1.** (A) Schematic of the experimental design of sample preparation, CZE-MS/MS
18 analysis, and database search. (B) schematic of the capillary inner-wall clean-up

1 procedure using NH₄OH. The figure is created using the BioRender and is used here with
2 permission.

3 Reproducibility of CZE-MS/MS for top-down proteomics of a complex sample

4 CZE-MS/MS with a fresh LPA-coated capillary generated reproducible measurements of
5 the yeast cell lysate, which is evidenced by the example electropherograms and the
6 number of proteoform identifications from the first roughly 10 runs, **Figures 2A** and **3A**.
7 When we kept running the yeast cell lysate, we observed that the proteoform peaks were
8 broadened gradually and proteoform intensity decreased accordingly, **Figure 2A**. The
9 peak width of one proteoform doubled in run 14 compared to that in run 1 and the
10 proteoform intensity decreased by a factor of two roughly. For runs 16, 22, and 23, the
11 peak width of the example proteoform tripled and the proteoform intensity is only 20% of
12 that in run 1. The number of proteoform and protein IDs decreased obviously from run 10
13 to run 24, **Figures 3A** and **3B**.

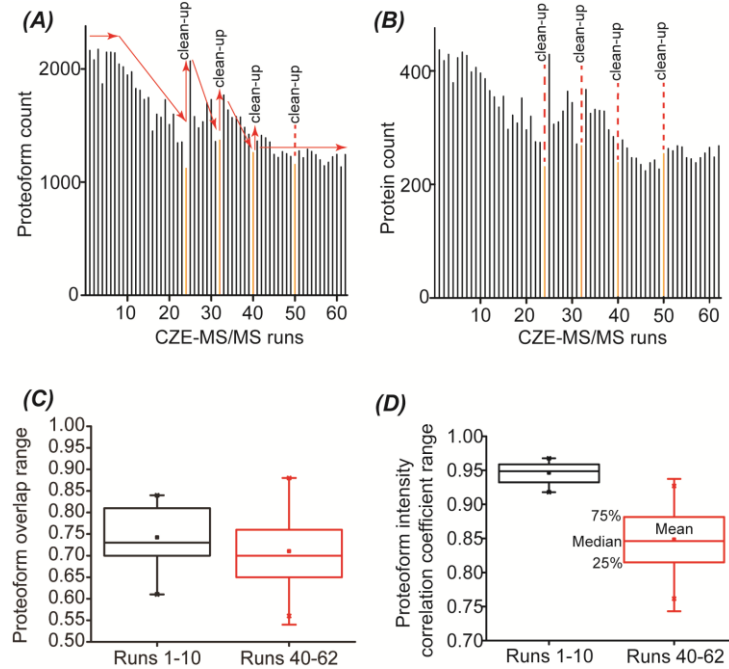


14
15 **Figure 2.** Electropherograms of a yeast cell lysate after analyses by CZE-MS/MS. (A)
16 Example runs during the first 23 CZE-MS/MS measurements. (B) Six example CZE-
17 MS/MS runs during the 40th to 62nd measurements.

1 We suspected that the phenomenon was due to proteoform adsorption onto the LPA
2 polymer coating on the capillary inner wall. When more and more CZE-MS/MS runs are
3 done, proteoforms are gradually adsorbed onto the capillary wall. The adsorbed
4 proteoforms can have significant impacts on CZE separation. Proteoforms on the capillary
5 inner wall are positively charged under the acidic BGE of 5% (v/v) acetic acid (pH 2.4),
6 leading to a potential of the generation of low reversed electroosmotic flow (EOF) in the
7 capillary. The reversed EOF slows down the migration of proteoforms in the capillary
8 and dispersion⁴³. The reversed EOF could also affect the performance of dynamic pH
9 junction stacking because it could negatively impact the migration of hydrogen protons
10 from the BGE vial to the separation capillary for sample zone titration.

11 **Figure S1B** shows an example electropherogram of the yeast cell lysate after over 30
12 continuous CZE-MS/MS runs without capillary cleanup. Once we cleaned up the capillary
13 inner wall using a procedure involving capillary flushing with 0.5% ammonium hydroxide,
14 water, and the BGE, the separation profile and the number of proteoform IDs recovered
15 back to nearly the original condition, **Figure S1A** and **S1C**. The data demonstrate that
16 the cleaning up method can remove the adsorbed proteoforms efficiently.

17 After the 1st and 2nd capillary cleanup, we observed the repeated phenomenon as the
18 fresh capillary. The number of proteoform and protein IDs declined as the runs continued,
19 **Figures 3A and 3B**. Interestingly, after the third cleanup, the capillary inner-wall condition
20 became more stable, evidenced by the relatively more consistent numbers of proteoform
21 and protein IDs (**Figures 3A and 3B**) as well as more reproducible proteoform
22 separations (**Figure 2B**). Our data suggest that to achieve reproducible top-down MS
23 measurements of a complex proteome sample by CZE-MS/MS, we can perform the
24 experiment either using a fresh LPA-coated capillary (Phase I) or using an LPA-coated
25 capillary after an enough amount of protein adsorption and sufficient capillary cleanup
26 with 0.5% ammonium hydroxide (Phase II). The phase II condition can provide
27 reproducible CZE-MS/MS measurements for more than 23 runs.



1

2 **Figure 3.** Summary of the identified proteoforms and proteins from 62 CZE-MS/MS runs.
3 (A) The number of proteoform IDs as a function of the run number. (B) The number of
4 protein IDs as a function of the run number. The trends of number of proteoform IDs and
5 the time for capillary cleanup are marked. (C) Boxplots of pairwise proteoform overlaps
6 for runs 1-10 and 40-62. (D) Boxplots of pairwise Pearson correlation coefficients of
7 proteoform intensity for runs 1-10 and 40-62. Log2 transformed proteoform intensities
8 were used to generate the Pearson correlation coefficients.

9 We further studied the pairwise overlap of identified proteoforms for phase I (runs 1-10)
10 and phase II (runs 40-62) conditions, **Figure 3C**. The medians of proteoform overlap
11 between any two CZE-MS/MS runs in phase I and phase II are both between 70%-75%,
12 which is comparable to CZE-MS/MS data in literatures⁴⁴. It documents that CZE-MS/MS
13 in both conditions can repeatedly identify the same proteoforms from the yeast cell lysate.
14 The small variations in the identified proteoforms are most likely due to the randomness
15 of data dependent acquisition (DDA).

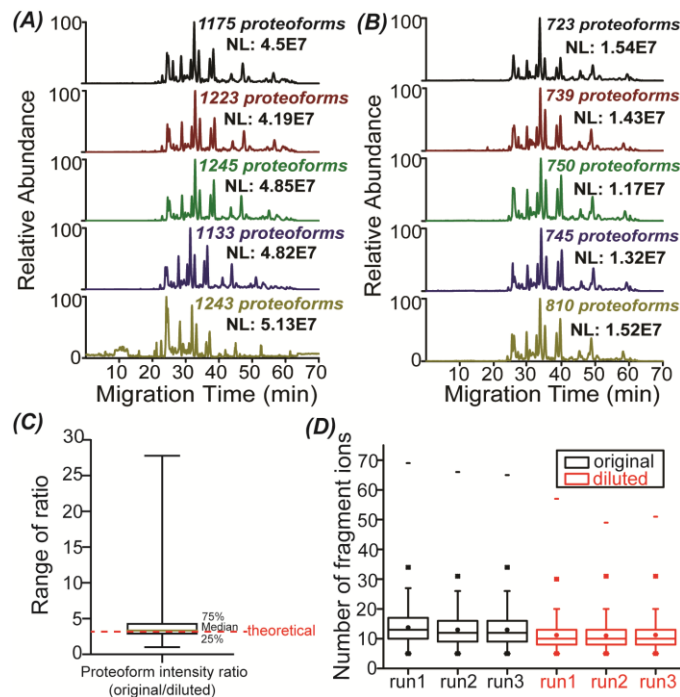
16 To investigate the quantitative reproducibility of CZE-MS/MS in both phase I and II
17 conditions, we studied the pairwise proteoform intensity correlation coefficients for runs
18 1-10 and 40-62, **Figure 3D**. Label free quantification of proteoforms was performed by

1 the TopDiff software⁴¹. The intensities of overlapped proteoforms between any two runs
2 were used to create the Pearson linear correlation and obtain the correlation coefficients.
3 The median for the phase I runs is about 0.95 and the correlation coefficient has a narrow
4 distribution, suggesting high quantitative reproducibility. The median for the phase II runs
5 is about 0.85, indicating reasonable quantitative reproducibility. The much lower Pearson
6 linear correlation coefficients in phase II runs than phase I runs are most likely due to
7 drastically lower proteoform intensities in phase II runs, as shown in **Figures 2A and 2B**.

8 To further confirm the possibility of CZE-MS/MS in the phase II condition for accurate
9 label-free quantification of proteoforms in a complex sample, after the 62 CZE-MS/MS
10 runs of the yeast cell lysate, we performed CZE-MS/MS analyses of a 3-times diluted
11 yeast cell lysate in quintuplicate, **Figure 4**. The CZE-MS/MS produced reproducible
12 measurements of the original and diluted yeast cell lysates in terms of separation profiles,
13 the number of proteoform IDs (1204±49 for original vs. 753±33 for diluted, relative
14 standard deviations (RSDs) as 4%, n=5), and the normalized level (NL) intensities (RSDs:
15 8%-9%, n=5), **Figures 4A and 4B**. The average NL intensity of the diluted sample is
16 about 3 times lower than that of the original sample (4.7E7 vs. 1.4E7), which agrees well
17 with the dilution factor of 3, demonstrating that the CZE-MS/MS in the phase II condition
18 performs well for relative quantification of proteoforms. We further analyzed the
19 distribution of proteoform intensity ratios between original and diluted samples, **Figure**
20 **4C**. The median of the ratios is close to the theoretical ratio of 3. The number of matched
21 fragment ions from the original sample is consistently higher than that from the diluted
22 sample, most likely due to the much higher proteoform intensity, **Figure 4D**. Majority of
23 the identified proteoforms have more than 10 matched fragment ions for the original and
24 diluted samples, indicating reasonably high confidence of the proteoform IDs.

25 The results presented in this study are critically important for CZE-MS/MS for top-down
26 proteomics of complex samples. First, the data document that CZE-MS/MS using one
27 LPA-coated capillary can produce high-quality top-down proteomics data of a complex
28 proteome sample for at least 78 hours (67 runs and 70 minutes per run), indicating the
29 high robustness of the system. Second, the study provides us with rich experimental data
30 that can be extremely useful for pursuing a better understanding of CZE-MS for

1 proteoform separation and characterization. Third, the results demonstrate that CZE-
 2 MS/MS with an appropriate operational procedure (i.e., capillary cleanup) can generate
 3 highly reproducible separation and identification of proteoforms in a complex sample
 4 across dozens of runs. The CZE-MS/MS is ready for some important biological
 5 applications to discover potentially critical proteoforms in biological processes and
 6 diseases in a quantitative manner. Fourth, the data also highlights some potential
 7 challenges of CZE-MS/MS for large-scale top-down proteomics studies in the next step
 8 and point out some important directions to work on. For example, we need to make more
 9 effort to create more consistent capillary inner-wall chemistry during CZE-MS/MS runs,
 10 which will eventually make CZE-MS/MS a powerful and highly reproducible technique for
 11 large-scale top-down proteomics studies.



12

13 **Figure 4.** Comparisons of the original and diluted yeast cell lysate data from CZE-
 14 MS/MS analyses. (A) Base peak electropherograms of the original yeast cell lysate after
 15 CZE-MS/MS analyses in quintuplicate. (B) Base peak electropherograms of the 3-times
 16 diluted yeast cell lysate after CZE-MS/MS analyses in quintuplicate. (C) Boxplot of the
 17 intensity ratio of overlapped proteoforms between original and diluted yeast cell lysates.

1 (D) Boxplots of the number of matched fragment ions of identified proteoforms from
2 original and diluted yeast samples.

3 **Correlation of experimental and predicted electrophoretic mobility of proteoforms
4 under different CZE-MS/MS conditions**

5 We have shown that the electrophoretic mobility (μ_{ef}) of proteoforms in CZE can be
6 predicted well using a simple semiempirical model^{21,45}. Proteoforms' experimental and
7 predicted μ_{ef} have high linear correlation coefficients. This feature is critically useful for
8 validating the proteoform IDs and the PTMs (i.e., phosphorylation). Here we have
9 multiple different CZE-MS/MS conditions, phase I (runs 1-10), phase II (runs 40-62),
10 and transition period between them (runs 11-39). We are asking how those CZE-
11 MS/MS conditions influence the correlation of experimental and predicted μ_{ef} of
12 proteoforms.

13 For the experimental μ_{ef} ($\text{cm}^2 \cdot \text{kV}^{-1} \cdot \text{s}^{-1}$), we used the equation 1 for calculation.

14 Experimental $\mu_{ef} = L / ((30-2) / L * t_M)$ (eq. 1)

15 Where L is the capillary length in cm, and t_M is the migration time in seconds. 30 and 2
16 are the separation voltage and electrospray voltage in kilovolts, respectively.

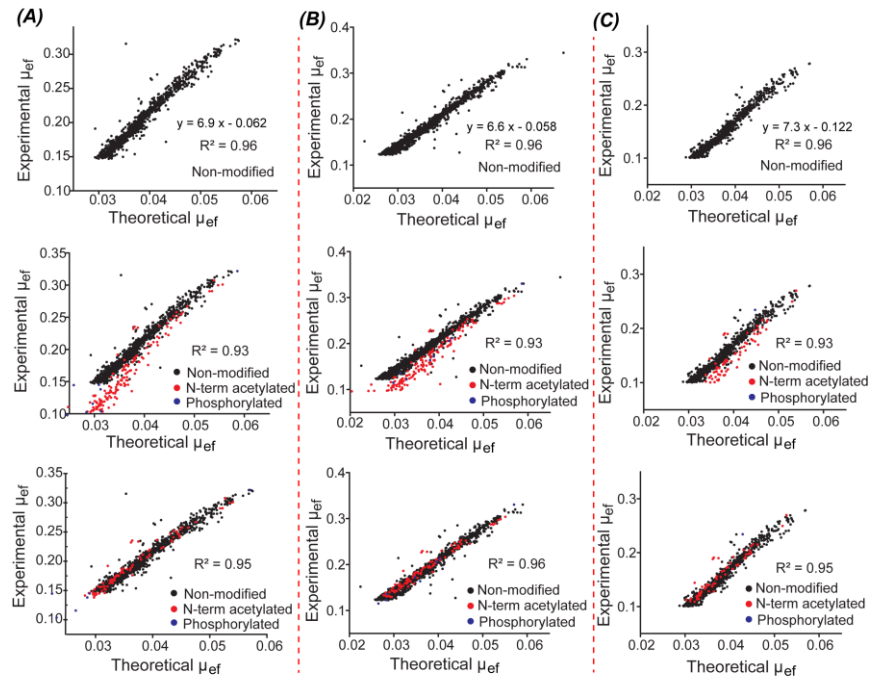
17 For the predicted μ_{ef} ($\text{cm}^2 \cdot \text{kV}^{-1} \cdot \text{s}^{-1}$), we utilized the equation 2.

18 Predicted $\mu_{ef} = \ln (1 + 0.35 * Q) / M^{0.411}$ (eq. 2)

19 Where M and Q represent molecular mass and charge number of each proteoform,
20 respectively. We got the information of M directly from the database search results. We
21 obtained Q by counting the number of lysine, arginine, and histidine amino acid residues
22 in the proteoform sequence and added 1 for the N-terminus.

23 We only used proteoforms containing no PTMs and those having N-terminal acetylation
24 or phosphorylation for this study. As shown in **Figures 5 A-C** (top panels), strong linear
25 correlations between experimental and predicted μ_{ef} were observed for proteoforms
26 without any PTMs ($R^2=0.96$). As shown in the middle panels, when we consider the

1 proteoforms with N-terminal acetylation or phosphorylation, those modified proteoforms
 2 fall off the main trend and have lower experimental μ_{ef} compared to the corresponding
 3 non-modified proteoforms. The reduction of experimental μ_{ef} is due to the charge (Q)
 4 reduction by one from the N-terminal acetylation or phosphorylation, considering the
 5 acidic BGE of CZE (i.e., 5% acetic acid, pH 2.4). After reducing the estimated net charge
 6 Q by one for the μ_{ef} prediction, we achieved strong linear correlation coefficients ($R^2=0.95$ -
 7 0.96) for the non-modified proteoforms and proteoforms having N-terminal acetylation or
 8 phosphorylation, **Figures 5 A-C** (bottom panels). The results here suggest that the
 9 proteoforms identified in this study have high confidence because of the strong linear
 10 correlations between experimental and predicted μ_{ef} . In addition, the data indicate that
 11 the different CZE-MS/MS conditions do not have significant impact on the correlations
 12 between experimental and predicted μ_{ef} . We realized that the experimental μ_{ef} of
 13 proteoforms become lower from run 5 (≥ 0.15 , **A**) to run 52 (≥ 0.1 , **C**), which is due to the
 14 much longer migration times of proteoforms in run 52 compared to run 5, **Figure 2**.



15
 16 **Figure 5.** Linear correlations between predicted μ_{ef} and experimental μ_{ef} of proteoforms
 17 from the yeast cell lysate identified in CZE-MS/MS run 5 (A), 25 (B), and run 52 (C). The
 18 top figures show the correlations for proteoforms without any PTMs. The middle ones

1 indicate the correlations for all proteoforms without PTMs and with N-terminal acetylation
2 or phosphorylation. The charge Q of those proteoforms were not corrected. The bottom
3 ones show the correlations for the same proteoforms as the middle ones but with charge
4 Q correction. For example, for one N-terminal acetylation or phosphorylation, the Q was
5 reduced by one.

6 **Conclusions**

7 For the first time, long-term qualitative and quantitative reproducibility of CZE-MS/MS for
8 a complex proteome sample was investigated. We revealed significant changes of
9 proteoforms in migration time and intensity after about 10 CZE-MS/MS runs of the yeast
10 cell lysate due to proteoform adsorption onto the capillary inner wall. We developed an
11 efficient and simple capillary cleanup procedure via flushing the capillary with 0.5%
12 NH₄OH, water, and the separation buffer successively. The capillary cleanup protocol can
13 remove the adsorbed proteoforms efficiently. After several rounds of capillary cleanup,
14 the capillary inner wall chemistry became more consistent, producing reproducible
15 proteoform separation and identification across dozens of CZE-MS/MS analyses of the
16 yeast cell lysate. The results in this work highlight that CZE-MS/MS is robust enough to
17 create high-quality top-down proteomics measurement of a complex sample across
18 dozens of runs, for example more than 60 runs of the yeast cell lysate. In addition, the
19 measurement can be qualitatively and quantitatively reproducible across dozens of runs
20 (i.e., at least 23 runs) under some specific condition with an appropriate operational
21 procedure (i.e., regular capillary cleanup). We expect that it is time to apply CZE-MS/MS-
22 based top-down proteomics to broad biological applications.

23 We have some recommendations about using CZE-MS for quantitative top-down
24 proteomics. For label-free quantification, we should not combine the Phase I and Phase
25 II conditions because of the dramatic shifts in migration time, making the data alignment
26 challenging across CZE-MS runs for relative quantification. If a small-scale label-free
27 quantification is performed, for example, comparing two samples with only about ten CZE-
28 MS runs or fewer, the Phase I condition will be ideal. If a large-scale study is needed, for
29 example, comparing multiple samples with more than 20 CZE-MS runs, the Phase II

1 condition should be considered. Alternatively, stable isotopic labeling techniques (e.g.,
2 tandem mass tags⁴⁶) can be employed. In this case, we may do not need to worry about
3 the Phase I or Phase II condition, because the relative quantification is performed based
4 on the data within the same CZE-MS runs.

5 **Supporting Information**

6 The following supporting information is available free of charge at ACS website.
7 Supporting Information 1: The lists of identified proteoforms from all CZE-MS/MS runs
8 (XLSX)
9 Supporting Information 2: Electropherograms of a yeast cell lysate by CZE-MS/MS in
10 three instances (PDF)

11 **Notes**

12 The authors declare no competing financial interest.

13 **Acknowledgments**

14 We thank the supports from the National Cancer Institute (NCI) through the grant
15 R01CA247863, the National Institute of General Medical Sciences (NIGMS) through
16 grants R01GM125991 and R01GM118470, and the National Science Foundation through
17 the grant DBI1846913 (CAREER Award).

18 **References**

19 [1] Toby, T. K.; Fornelli, L.; Kelleher, N. L. Progress in Top-Down Proteomics and the
20 Analysis of Proteoforms. *Annu. Rev. Anal. Chem.* **2016**, *9*, 499–519.

21 [2] Adams, L. M.; DeHart, C. J.; Drown, B. S.; Anderson, L. C.; Bocik, W.; Boja, E. S.;
22 Hiltke, T. M.; Hendrickson, C. L.; Rodriguez, H.; Caldwell, M.; Vafabakhsh, R.; Kelleher,
23 N. L. Mapping the KRAS proteoform landscape in colorectal cancer identifies truncated
24 KRAS4B that decreases MAPK signaling. *J. Biol. Chem.* **2023**, *299*, 102768.

1 [3] McCool, E. N.; Xu, T.; Chen, W.; Beller, N. C.; Nolan, S. M.; Hummon, A. B.; Liu, X.;
2 Sun, L. Deep Top-down Proteomics Revealed Significant Proteoform-Level Differences
3 between Metastatic and Nonmetastatic Colorectal Cancer Cells. *Sci. Adv.* **2022**, *8*,
4 eabq6348.

5 [4] Ntai, I.; LeDuc, R. D.; Fellers, R. T.; Erdmann-Gilmore, P.; Davies, S. R.; Rumsey, J.;
6 Early, B. P.; Thomas, P. M.; Li, S.; Compton, P. D.; Ellis, M. J. C.; Ruggles, K. V.; Fenyö,
7 D.; Boja, E. S.; Rodriguez, H.; Townsend, R. R.; Kelleher, N. L. Integrated Bottom-Up and
8 Top-Down Proteomics of Patient-Derived Breast Tumor Xenografts. *Mol. Cell.*
9 *Proteomics* **2016**, *15*, 45-56.

10 [5] Ntai, I.; Fornelli, L.; DeHart, C. J.; Hutton, J. E.; Doubleday, P. F.; LeDuc, R. D.; Nispen,
11 A. J. van.; Fellers, R. T.; Whiteley, G.; Boja, E. S.; Rodriguez, H.; Kelleher, N. L. Precise
12 characterization of KRAS4b proteoforms in human colorectal cells and tumors reveals
13 mutation/modification cross-talk. *Proc. Natl. Acad. Sci. USA* **2018**, *115*, 4140-4145.

14 [6] Kandi, S.; Cline, E. N.; Rivera, B. M.; Viola, K. L.; Zhu, J.; Condello, C.; LeDuc, R. D.;
15 Klein, W. L.; Kelleher, N. L.; Patrie, S. M. Amyloid β Proteoforms Elucidated by
16 Quantitative LC/MS in the 5xFAD Mouse Model of Alzheimer's Disease. *J. Proteome Res.*
17 **2023**, *22*, 3475-3488.

18 [7] Kellie, J. F.; Higgs, R. E.; Ryder, J. W.; Major, A.; Beach, T. G.; Adler, C. H.; Merchant,
19 K.; Knierman, M. D. Quantitative measurement of intact alpha-synuclein proteoforms from
20 post-mortem control and Parkinson's disease brain tissue by intact protein mass
21 spectrometry. *Sci. Rep.* **2014**, *4*, 5797.

22 [8] Schmitt, N. D.; Agar, J. N. Parsing disease-relevant protein modifications from
23 epiphenomena: perspective on the structural basis of SOD1-mediated ALS. *J. Mass*
24 *Spectrom.* **2017**, *52*, 480-491.

25 [9] Forgrave, L. M.; Moon, K. M.; Hamden, J. E.; Li, Y.; Lu, P.; Foster, L. J.; Mackenzie,
26 I. R. A.; DeMarco, M. L. Truncated TDP-43 proteoforms diagnostic of frontotemporal
27 dementia with TDP-43 pathology. *Alzheimers Dement.* **2023**, doi: 10.1002/alz.13368.

1 [10] Ge, Y.; Rybakova, I. N.; Xu, Q.; Moss, R. L. Top-down High-Resolution Mass
2 Spectrometry of Cardiac Myosin Binding Protein C Revealed That Truncation Alters
3 Protein Phosphorylation State. *Proc. Natl. Acad. Sci. USA* **2009**, *106*, 12658–12663.

4 [11] Chamot-Rooke, J.; Mikaty, G.; Malosse, C.; Soyer, M.; Dumont, A.; Gault, J.; Imhaus,
5 A.-F.; Martin, P.; Trellet, M.; Clary, G.; Chafey, P.; Camoin, L.; Nilges, M.; Nassif, X.;
6 Duménil, G. Posttranslational Modification of Pili upon Cell Contact Triggers N.
7 Meningitidis Dissemination. *Science* **2011**, *331*, 778–782.

8 [12] Roberts, D. S.; Mann, M.; Melby, J. A.; Larson, E. J.; Zhu, Y.; Brasier, A. R.; Jin, S.;
9 Ge, Y. Structural O-Glycoform Heterogeneity of the SARS-CoV-2 Spike Protein
10 Receptor-Binding Domain Revealed by Top-Down Mass Spectrometry. *J. Am. Chem.
11 Soc.* **2021**, *143*, 12014-12024.

12 [13] Gstottnar, C.; Zhang, T.; Resemann, A.; Ruben, S.; Pengelley, S.; Suckau, D.;
13 Welsink, T.; Wührer, M.; Domínguez-Vega, E. Structural and functional characterization
14 of SARS-CoV-2 RBD domains produced in mammalian cells. *Anal. Chem.* **2021**, *93*,
15 6839-6847.

16 [14] Wilson, J. W.; Bilbao, A.; Wang, J.; Liao, Y. C.; Velickovic, D.; Wojcik, R.; Passamonti,
17 M.; Zhao, R.; Gargano, A. F. G.; Gerbasi, V. R.; Pas A-Tolić, L.; Baker, S. E.; Zhou, M.
18 Online hydrophilic interaction chromatography (HILIC) enhanced top-down mass
19 spectrometry characterization of the SARS-CoV-2 spike receptor-binding domain. *Anal.
20 Chem.* **2022**, *94*, 5909-5917.

21 [15] Melani, R. D.; Des Soye, B. J.; Kafader, J. O.; Forte, E.; Hollas, M.; Blagojevic, V.;
22 Negrão, F.; McGee, J. P.; Drown, B.; Lloyd-Jones, C.; Seckler, H. S.; Camarillo, J. M.;
23 Compton, P. D.; LeDuc, R. D.; Early, B.; Fellers, R. T.; Cho, B. K.; Mattamana, B. B.;
24 Goo, Y. A.; Thomas, P. M.; Ash, M. K.; Bhimalli, P. P.; Al-Harthi, L.; Sha, B. E.; Schneider,
25 J. R.; Kelleher, N. L. Next-generation serology by mass spectrometry: readout of the
26 SARS-CoV-2 antibody repertoire. *J. Proteome Res.* **2021**, *21*, 274-288.

1 [16] Brown, K. A.; Melby, J. A.; Roberts, D. S.; Ge, Y. Top-down proteomics: challenges,
2 innovations, and applications in basic and clinical research. *Expert Rev. Proteomics*
3 **2020**, *17*, 719-733.

4 [17] Schaffer, L. V.; Millikin, R. J.; Miller, R. M.; Anderson, L. C.; Fellers, R. T.; Ge, Y.;
5 Kelleher, N. L.; LeDuc, R. D.; Liu, X.; Payne, S. H.; Sun, L.; Thomas, P. M.; Tucholski, T.;
6 Wang, Z.; Wu, S.; Wu, Z.; Yu, D.; Shortreed, M. R.; Smith, L. M. Identification and
7 Quantification of Proteoforms by Mass Spectrometry. *Proteomics* **2019**, *19*, e1800361.

8 [18] Lukacs, K. D.; Jorgenson, J. W. Capillary Zone Electrophoresis. *Science* **1983**, *222*,
9 266-272.

10 [19] Chen, D.; McCool, E. N.; Yang, Z.; Shen, X.; Lubeckyj, R. A.; Xu, T.; Wang, Q.; Sun,
11 L. Recent Advances (2019–2021) of Capillary Electrophoresis-Mass Spectrometry for
12 Multilevel Proteomics. *Mass Spectrom Rev* **2023**, *42*, 617–642.

13 [20] Shen, X.; Yang, Z.; McCool, E. N.; Lubeckyj, R. A.; Chen, D.; Sun, L. Capillary zone
14 electrophoresis-mass spectrometry for top-down proteomics. *Trends Analyt. Chem.*
15 **2019**, *120*, 115644.

16 [21] Chen, D.; Lubeckyj, R. A.; Yang, Z.; McCool, E. N.; Shen, X.; Wang, Q.; Xu, T.; Sun,
17 L. Predicting Electrophoretic Mobility of Proteoforms for Large-Scale Top-Down
18 Proteomics. *Anal Chem* **2020**, *92*, 3503–3507.

19 [22] Valaskovic, G. A.; Kelleher, N.L.; McLafferty, F. W. Attomole protein characterization
20 by capillary electrophoresis-mass spectrometry. *Science* **1996**, *273*, 1199-1202.

21 [23] Akashi, S.; Suzuki, K.; Arai, A.; Yamada, N.; Suzuki, E.; Hirayama, K.; Nakamura,
22 S.; Nishimura, Y. Top-down analysis of basic proteins by microchip capillary
23 electrophoresis mass spectrometry. *Rapid Commun. Mass Spectrom.* **2006**, *20*, 1932-
24 38.

25 [24] Han, X.; Wang, Y.; Aslanian, A.; Bern, M.; Lavallée-Adam, M.; Yates, J. R.
26 Sheathless capillary electrophoresis-tandem mass spectrometry for top-down

1 characterization of *Pyrococcus furiosus* proteins on a proteome scale. *Anal. Chem.* **2014**,
2 86, 11006-11012.

3 [25] Zhao, Y.; Sun, L.; Zhu, G.; Dovichi, N. J. Coupling capillary zone electrophoresis to
4 a Q exactive HF mass spectrometer for top-down proteomics: 580 proteoform
5 identifications from yeast. *J. Proteome Res.* **2016**, 15, 3679-3685.

6 [26] Lubeckyj, R. A.; McCool, E. N.; Shen, X.; Kou, Q.; Liu, X.; Sun, L. Single-Shot Top-
7 Down Proteomics with Capillary Zone Electrophoresis-Electrospray Ionization-Tandem
8 Mass Spectrometry for Identification of Nearly 600 *Escherichia Coli* Proteoforms. *Anal*
9 *Chem* **2017**, 89, 12059–12067.

10 [27] Xu, T.; Wang, Q.; Wang, Q.; Sun, L. Coupling High-Field Asymmetric Waveform Ion
11 Mobility Spectrometry with Capillary Zone Electrophoresis-Tandem Mass Spectrometry
12 for Top-Down Proteomics. *Anal. Chem.* **2023**, 95, 9497–9504.

13 [28] Wang, Q.; Fang, F.; Wang, Q.; Sun, L. Capillary zone electrophoresis-high field
14 asymmetric ion mobility spectrometry-tandem mass spectrometry for top-down
15 characterization of histone proteoforms. *Proteomics* **2023**, e2200389.

16 [29] Wang, Q.; Xu, T.; Fang, F.; Wang, Q.; Lundquist, P.; Sun, L. Capillary Zone
17 Electrophoresis-Tandem Mass Spectrometry for Top-Down Proteomics of Mouse Brain
18 Integral Membrane Proteins. *Anal. Chem.* **2023**, 95, 12590–12594.

19 [30] Drown, B. S.; Jooß, K.; Melani, R. D.; Lloyd-Jones, C.; Camarillo, J. M.; Kelleher, N.
20 L. Mapping the Proteoform Landscape of Five Human Tissues. *J. Proteome Res.* **2022**,
21 21, 1299–1310.

22 [31] Johnson, K. R.; Gao, Y.; Greguš, M.; Ivanov, A. R. On-Capillary Cell Lysis Enables
23 Top-down Proteomic Analysis of Single Mammalian Cells by CE-MS/MS. *Anal. Chem.*
24 **2022**, 94, 14358–14367.

25 [32] Zhu, G.; Sun, L.; Dovichi, N. J. Thermally-Initiated Free Radical Polymerization for
26 Reproducible Production of Stable Linear Polyacrylamide Coated Capillaries, and Their

1 Application to Proteomic Analysis Using Capillary Zone Electrophoresis-Mass
2 Spectrometry. *Talanta* **2016**, *146*, 839–843.

3 [33] Sun, L.; Zhu, G.; Zhao, Y.; Yan, X.; Mou, S.; Dovichi, N. J. Ultrasensitive and Fast
4 Bottom-up Analysis of Femtogram Amounts of Complex Proteome Digests. *Angew. Chem Int. Ed.* **2013**, *52*, 13661-4.

5 [34] Wojcik, R.; Dada, O. O.; Sadilek, M.; Dovichi, N. J. Simplified Capillary
6 Electrophoresis Nanospray Sheath-Flow Interface for High Efficiency and Sensitive
7 Peptide Analysis. *Rapid Commun. Mass Spectrom.* **2010**, *24*, 2554–2560.

8 [35] Sun, L.; Zhu, G.; Zhang, Z.; Mou, S.; Dovichi, N. J. Third-Generation Electrokinetically
9 Pumped Sheath-Flow Nanospray Interface with Improved Stability and Sensitivity for
10 Automated Capillary Zone Electrophoresis-Mass Spectrometry Analysis of Complex
11 Proteome Digests. *J. Proteome Res.* **2015**, *14*, 2312–2321.

12 [36] Kou, Q.; Xun, L.; Liu, X. TopPIC: A Software Tool for Top-down Mass Spectrometry-
13 Based Proteoform Identification and Characterization. *Bioinformatics* **2016**, *32*, 3495–
14 3497.

15 [37] Kessner, D.; Chambers, M.; Burke, R.; Agus, D.; Mallick, P. ProteoWizard: Open
16 Source Software for Rapid Proteomics Tools Development. *Bioinformatics* **2008**, *24*,
17 2534–2536.

18 [38] Basharat, A. R.; Zang, Y.; Sun, L.; Liu, X. TopFD: A Proteoform Feature Detection
19 Tool for Top-Down Proteomics. *Anal. Chem.* **2023**, *95*, 8189–8196.

20 [39] Keller, A.; Nesvizhskii, A. I.; Kolker, E.; Aebersold, R. Empirical Statistical Model to
21 Estimate the Accuracy of Peptide Identifications Made by MS/MS and Database Search.
22 *Anal. Chem.* **2002**, *74*, 5383–5392.

23 [40] Elias, J. E.; Gygi, S. P. Target-Decoy Search Strategy for Increased Confidence in
24 Large-Scale Protein Identifications by Mass Spectrometry. *Nat. Methods* **2007**, *4*, 207–
25 214.

1 [41] Lubeckyj, R. A.; Basharat, A. R.; Shen, X.; Liu, X.; Sun, L. Large-Scale Qualitative
2 and Quantitative Top-Down Proteomics Using Capillary Zone Electrophoresis-
3 Electrospray Ionization-Tandem Mass Spectrometry with Nanograms of Proteome
4 Samples. *J. Am. Soc. Mass Spectrom.* **2019**, *30*, 1435–1445.

5 [42] Perez-Riverol, Y.; Csordas, A.; Bai, J.; Bernal-Llinares, M.; Hewapathirana, S.;
6 Kundu, D. J.; Inuganti, A.; Griss, J.; Mayer, G.; Eisenacher, M.; Pérez, E.; Uszkoreit, J.;
7 Pfeuffer, J.; Sachsenberg, T.; Yilmaz, S.; Tiwary, S.; Cox, J.; Audain, E.; Walzer, M.;
8 Jarnuczak, A. F.; Ternent, T.; Brazma, A.; Vizcaíno, J. A. The PRIDE Database and
9 Related Tools and Resources in 2019: Improving Support for Quantification Data. *Nucleic
10 Acids Res.* **2019**, *47*, D442–D450.

11 [43] Khodabandehloo, A.; Chen, D. D. Y. Electroosmotic Flow Dispersion of Large
12 Molecules in Electrokinetic Migration. *Anal. Chem.* **2017**, *89*, 7823–7827.

13 [44] McCool, E. N.; Lubeckyj, R. A.; Shen, X.; Chen, D.; Kou, Q.; Liu, X.; Sun, L. Deep
14 Top-Down Proteomics Using Capillary Zone Electrophoresis-Tandem Mass
15 Spectrometry: Identification of 5700 Proteoforms from the Escherichia Coli Proteome.
16 *Anal. Chem.* **2018**, *90*, 5529–5533.

17 [45] Chen, D.; Yang, Z.; Shen, X.; Sun, L. Capillary Zone Electrophoresis-Tandem Mass
18 Spectrometry As an Alternative to Liquid Chromatography-Tandem Mass Spectrometry
19 for Top-down Proteomics of Histones. *Anal. Chem.* **2021**, *93*, 4417–4424.

20 [46] Guo, Y.; Chowdhury, T.; Seshadri, M.; Cupp-Sutton, K. A.; Wang, Q.; Yu, D.; Wu, S.
21 Optimization of Higher-Energy Collisional Dissociation Fragmentation Energy for Intact
22 Protein-Level Tandem Mass Tag Labeling. *J. Proteome Res.* **2023**, *22*, 1406-1418.

23

24

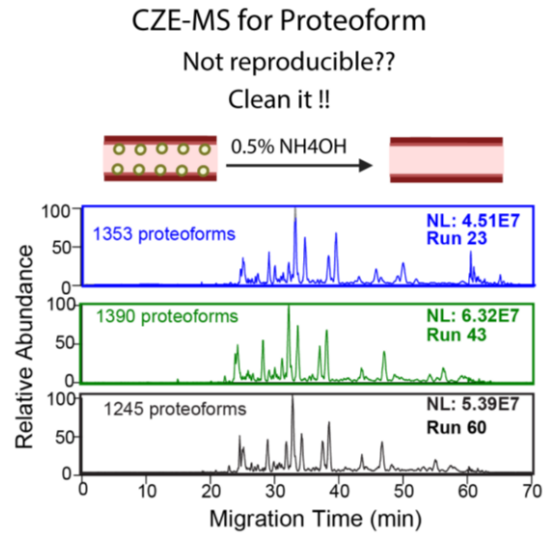
25

26

1

2

3 For TOC Only



4

5

6